Determination of the Amide-Plane Orientations in a Cyclo-β-Peptide by Magic-Angle-Spinning Deuterium-Correlation Spectroscopy, and Comparison with the Powder X-Ray Structure

by **Hongbiao C. Le**[a])[1]), **Tobias Hintermann**[b]), **Thomas Wessels**[c]), **Zhehong Gan**[a])[2]), **Dieter Seebach**[b]), and **Richard R. Ernst***[a])

[a]) Laboratorium für Physikalische Chemie, Eidgenössische Technische Hochschule, ETH-Zentrum, Universitätstrasse 22, CH-8092 Zürich

[b]) Laboratorium für Organische Chemie, Eidgenössische Technische Hochschule, ETH-Zentrum, Universitätstrasse 16, CH-8092 Zürich

[c]) Laboratorium für Kristallographie, Eidgenössische Technische Hochschule, ETH-Zentrum, Sonneggstrasse 5, CH-8092, Zürich, Switzerland

Previously, it has been shown that the correlation of deuterium quadrupolar tensors by spin diffusion under slow magic-angle-spinning conditions can provide accurate measurements of their relative orientation. In the present work we apply the technique to the cyclo-β-peptide cyclo[(*S*)-β-homoalanyl-(*R*)-β-homoalanyl-(*S*)-β-homoalanyl-(*R*)-β-homoalanyl] with its amide hydrogens labeled by deuterons. From the 2D spin-diffusion spectrum, it is possible to determine the mutual orientation of the amide deuteron quadrupolar coupling tensors. Assuming that the molecule has four-fold molecular symmetry, the polar angles of the symmetry axis in the principal-axis frames of the deuterium electric-field-gradient tensors are found to be $\theta = 15.7^\circ \pm 1.0^\circ$ or $\theta = 164.3^\circ \pm 1.0^\circ$, and $\phi = \pm 72^\circ \pm 10^\circ$. They are used to deduce possible conformations of the peptide based on the result of a previous measurement that correlated the deuterium principal quadrupolar frame with a local molecular frame. We found eight conformations that are all consistent with the NMR measurement. Three of these have acceptably small *van der Waals* contact energies. One of the three structures agrees, within a rmsd of 6° for the backbone dihedral angles, with an X-ray conformation.

Introduction. – NMR Spectroscopy has become an indispensible tool for the structural and dynamical studies of molecules ranging from small organic molecules to large biomolecules [1–5]. With solid-state NMR techniques, it is possible to measure geometric parameters, such as the distance between two isotopically labeled sites and the relative orientation of their principle axis frames [6–9]. These techniques exploit the distance-dependent dipolar coupling and also the orientation-dependent dipolar, anisotropic chemical shift, and quadrupolar interactions. To obtain angular information, one can correlate two spatially anisotropic interactions, such as the combinations dipole-dipole [10], dipole-CSA [11], CSA-CSA [12], and quadrupole-quadrupole [13] (CSA = chemical shielding anisotropy). ^{2}H-Atoms incorporated into (bio)molecules are good candidates for the application of quadrupolar correlation techniques. ^{2}H-Quadrupolar-coupling frequencies range from 10 to 270 kHz, making them readily accessible to various spectral manipulations. The spin diffusion between nuclei with

[1]) Current address: Biomedical Magnetic Resonance Laboratory, University of Illinois, 2100 S Goodwin Ave., Urbana, IL 61801, USA

[2]) Current address: Center of Interdisciplinary Magnetic Resonance, National High Magnetic Field Laboratory, Tallahassee, Florida 32306-4005, USA

largely different quadrupolar interactions can be enhanced by angular sample hopping or spinning [13][14].

Recently, there has been great interest in searching for and studying non-naturally occurring heteropolymers that may possess structures resembling those of α-peptides and nucleotides, and that may be biologically active. These, unlike α-peptides, adopt highly-structured conformations, even with very few residues [15]. The conformational analysis was generally carried out by means of X-ray diffraction and solution NMR [16]. Because it is difficult to grow single crystals of β-peptides suitable for X-ray diffraction, solid-state NMR of powder samples may be an attractive choice.

In the present study, ^{2}H spin-diffusion spectroscopy is applied to the cyclo-β-peptide cyclo[(*S*)-β-homoalanyl-(*R*)-β-homoalanyl-(*S*)-β-homoalanyl-(*R*)-β-homoalanyl] **1** (*Fig. 1,a*) for determining the amide-plane orientations and obtaining information on the molecular structure. The structural analysis of **1** is simplified due to the S_4 molecular symmetry. The results are compared with those of a X-ray powder-diffraction study.

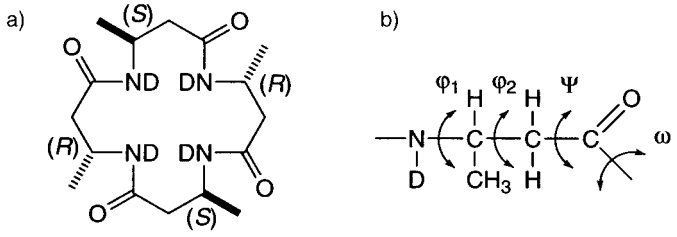

1

Fig. 1. a) *Cyclo-β-peptide cyclo[(*S*)-β-homoalanyl-(*R*)-β-homoalanyl-(*S*)-β-homoalanyl-(*R*)-β-homoalanyl]* (**1**). b) *Definition of the backbone dihedral angles* φ_1, φ_2, ψ, *and* ω *for a monomer unit*. Dihedral angles are measured between the backbone bonds.

Theory. – *Two-Dimensional ^{2}H Spin-Diffusion Spectroscopy.* The *Hamiltonian* of a ^{2}H spin-pair under magic-angle sample spinning with quadrupolar interaction, chemical-shift interaction, and the dipolar interaction between the two nuclei is

$$H(t) = \mathrm{q}_1(t)(\mathrm{S}_{1z}^2 - \mathbf{S}_1^2/3) + \mathrm{q}_2(t)(\mathrm{S}_{2z}^2 - \mathbf{S}_2^2/3) + \Omega_1(t)\mathrm{S}_{1z} + \Omega_2(t)\mathrm{S}_{2z} + \mathrm{d}_{12}(t)[2\mathrm{S}_{1z}\mathrm{S}_{2z} - (\mathrm{S}_1^+\mathrm{S}_2^- - \mathrm{S}_1^-\mathrm{S}_2^+)/2]. \quad (1)$$

Here, $\mathrm{q}_1(t)$, $\mathrm{q}_2(t)$ denote the time-modulated quadrupolar coupling frequencies for the two deuterons, $\Omega_1(t)$, $\Omega_2(t)$ the chemical shifts, and $\mathrm{d}_{12}(t)$ the dipolar coupling frequency.

During the free-precession periods t_1 and t_2 of the two-dimensional (2D) spin-diffusion experiment of *Fig. 2* [14], the transverse magnetization evolves primarily under the quadrupolar interaction, while chemical shift and dipolar interactions are small in comparison and can be ignored. During the mixing period τ_m, sample spinning induces exchange of polarization between two spins *via* dipolar coupling. The phase cycling scheme selects the exchange of *Zeeman* order.

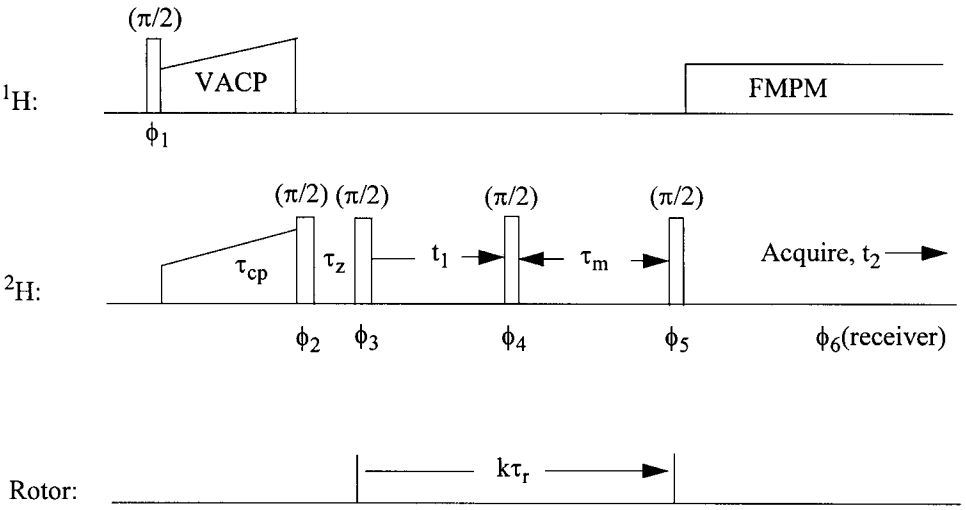

Fig. 2. *Pulse sequence for 2D ^{2}H spin-diffusion spectra.* The initial polarization of ^{2}H from ^{1}H employs variable amplitude cross-polarization (VACP). It is followed by a z-filter period of duration τ_z for allowing the excitation pulse, starting the modulation period t_1, to be synchronized with the MAS rotor phase. Also the second mixing pulse, initiating the detection period, is synchronized. ^{1}H-Decoupling during detection uses the sequence FMPM (Freqency-Modulation Phase-Modulation) [24]. The following 16-step phase cycling is applied: $\phi_1 = (-x, x)_8$; $\phi_2 = (y)_{16}$; $\phi_3 = (x)_8, (-x)_8$; $\phi_4 = (-x)_{16}$; $\phi_5 = ((x)_2, (y)_2, (-x)_2, (-y)_2)_2$; $\phi_6 = -x, x, -y, y, x, -x, y, -y, x, -x, y, -y, -x, x, -y, y$. Cross-polarization uses y and x phases for ^{1}H and ^{2}H, respectively.

The 2D time-domain signal of N dipolar-coupled deuterons can be expressed by

$$S(t_1,t_2,\tau_m) = \sum_{i,j=1}^{N} S_{ij}(t_1,t_2,\tau_m) \tag{2}$$

where S_{ij} is the contribution of polarization transfer from the deuteron spin i to spin j with

$$S_{ij}(t_1,t_2,\tau_m) = A_{ij}(\tau_m)\cos\phi_i(0,t_1)\cos\phi_j(t_1+\tau_m, t_1+\tau_m+t_2). \tag{3}$$

The dynamic phase angle $\phi_i(t', t'')$ is determined by the time-dependent quadrupolar-interaction frequency $q_i(t)$

$$\phi_i(t',t'') = \int_{t'}^{t''} q_i(t)dt \tag{4}$$

where t' and t'' are the starting and ending time, respectively, of the free precession of the transverse magnetization under the influence of quadrupolar interaction. $A_{ij}(\tau_m)$ is the polarization-transfer amplitude from deuteron spin i to j during the mixing period τ_m [14]. On a time-scale short compared to the relaxation time T_1, the total polarization originating from spin i is conserved:

$$\sum_{j=1}^{N} A_{ij}(\tau_m) = 1. \tag{5}$$

An equal distribution of polarization is achieved asymptotically, when the polarization exchange is much faster than T_1 relaxation:

$$A_{ij}(\tau_m \approx \infty) = \frac{1}{N}. \quad (6)$$

For a powder sample, the observed 2D FID signal is obtained by averaging *Eqn. 2* over all possible molecular orientations.

For eliminating the dependence of the dynamic phase angles ϕ_i and ϕ_j on the mixing time τ_m, rotor synchronization of the mixing pulses, as indicated in the pulse sequence in *Fig. 2*, is necessary. With the rotor synchronization condition, $t_1 + \tau_m = k\tau_r$, where k is a positive integer and τ_r is the rotor period, *Eqn. 3* can be rewritten as

$$S_{ij}(t_1, t_2, \tau_m) = A_{ij}(\tau_m)(\cos\phi_i(0, t_1)\cos\phi_j(0, t_2)). \quad (7)$$

Eqns. 2, *6*, and *7* form the basis for the computer simulation and the fitting of the measured 2D time-domain signal and for the determination of the relative quadrupolar tensor orientation.

Structural Analysis. The cyclo-β-tetrapeptide **1** under investigation consists of two (R)- and two (S)-β-homoalanyl residues (β-HAla). Assuming standard bond lengths, bond angles, and free rotation of the Me groups, its structure is completely defined by the four dihedral angles φ_1^i, φ_2^i, ψ^i, and ω^i of each residue i, which are defined as shown in *Fig. 1,b*. Its symmetrical composition leads to a geometry of S_4 symmetry. The dihedral angles φ_1^i, φ_2^i, ψ^i, and ω^i of consecutive residues are, therefore, equal in magnitude but of opposite sign. In addition, a closure relationship for the 16 consecutive backbone vectors $\mathbf{v}_i$ of the cyclic peptide must apply:

$$\sum_{i=1}^{16} \mathbf{v}_i = 0. \quad (8)$$

With this constraint, the total number of free dihedral angles is reduced to three. In addition, the assumption that the amide moieties adopt a planar conformation, $\omega = 180°$, makes the complete peptide conformation depend on only two angular parameters.

The NMR measurement does not provide direct geometric information, but allows one to determine the mutual orientation of the four quadrupolar-coupling tensors. Because of the molecular S_4 symmetry, it is uniquely defined by the orientation of the S_4 symmetry axis in the quadrupolar principal axis frame of residue i with the polar angles θ_q^i and ϕ_q^i and the relations $\theta_q^{i+1} = 180° - \theta_q^i$ and $\phi_q^{i+1} = -\phi_q^i$ (*Fig. 3,a*).

When the orientation of the quadrupolar tensor in a molecular frame is known, also geometric information can be deduced. It is known that the peptide moiety, consisting of the five nuclei CONDC$_\alpha$, is nearly planar. *Gerald et al.* measured the amide ^{2}H quadrupolar-coupling tensor and its orientation in a *N*-acetylvaline single crystal [17]. Their measurement showed that V_{zz}-axis is 1.8° off the N–^{2}H bond while V_{xx}-axis is 0.9° off the amide plane normal. Within our measurement accuracy, these deviations are negligible, and we assume V_{zz} to be parallel to the N–^{2}H bond and V_{xx} perpendicular to the amide plane (*Fig. 3,b*). This fixes together with quadrupolar tensor also the orientation of the peptide planes relative to the S_4 symmetry axis.

With a fixed orientation of the peptide planes, there is, in general, a finite number of compatible backbone geometries with the dihedral angles φ_1^i, φ_2^i and ψ^i. Except for special values of θ_q^i and ϕ_q^i, there are eight possible backbone geometries leading to the same relative orientation of the peptide planes. Because no convenient analytical

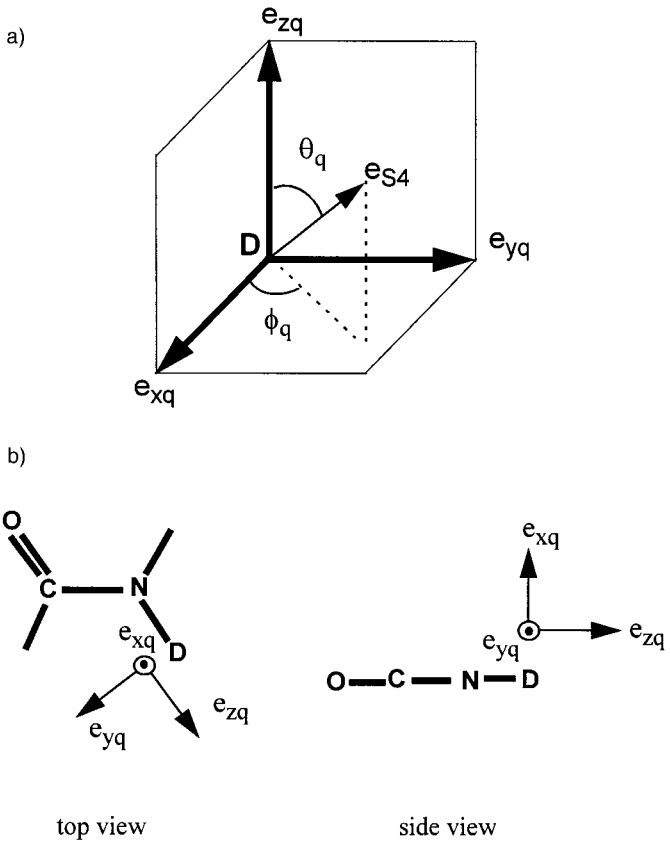

Fig. 3. a) *Orientation of symmetry axis* e_{S_4} *in the quadrupolar principal-axis frame* e_{xq}, e_{yq}, e_{zq} *with the polar angles* θ_q and ϕ_q. b) *Assumed orientation of the quadrupolar principal-axis frame with respect to the peptide plane.*

relationship between θ_q^i and ϕ_q^i, and the backbone dihedral angles φ_1^i, φ_2^i, and ψ^i exists, it is best to apply an iterative or graphical method for the determination of the backbone dihedral angles.

To select the most likely one of the eight compatible molecular structures, additional information obtained from other sources must be used. It is, for example, possible to rate the structures based on their *van der Waals* interaction energies, which can be computed by one of the well-known mechanical force fields, such as AMBER [18][19].

Results and Discussion. – *Fig. 4,a*, shows the 2D time-domain data for 7 s of spin diffusion in the cyclo-β-peptide **1**. At this time, the system was found to be close to a quasi-equilibrium state with stationary signal intensities. Data points from a single rotor period in t_1 and t_2 dimensions are shown, since time-domain data are the product of a function periodic with the rotor frequency and a relaxation decay function in both dimensions. The sharp peak in the center of the plot is the rotational echo peak.

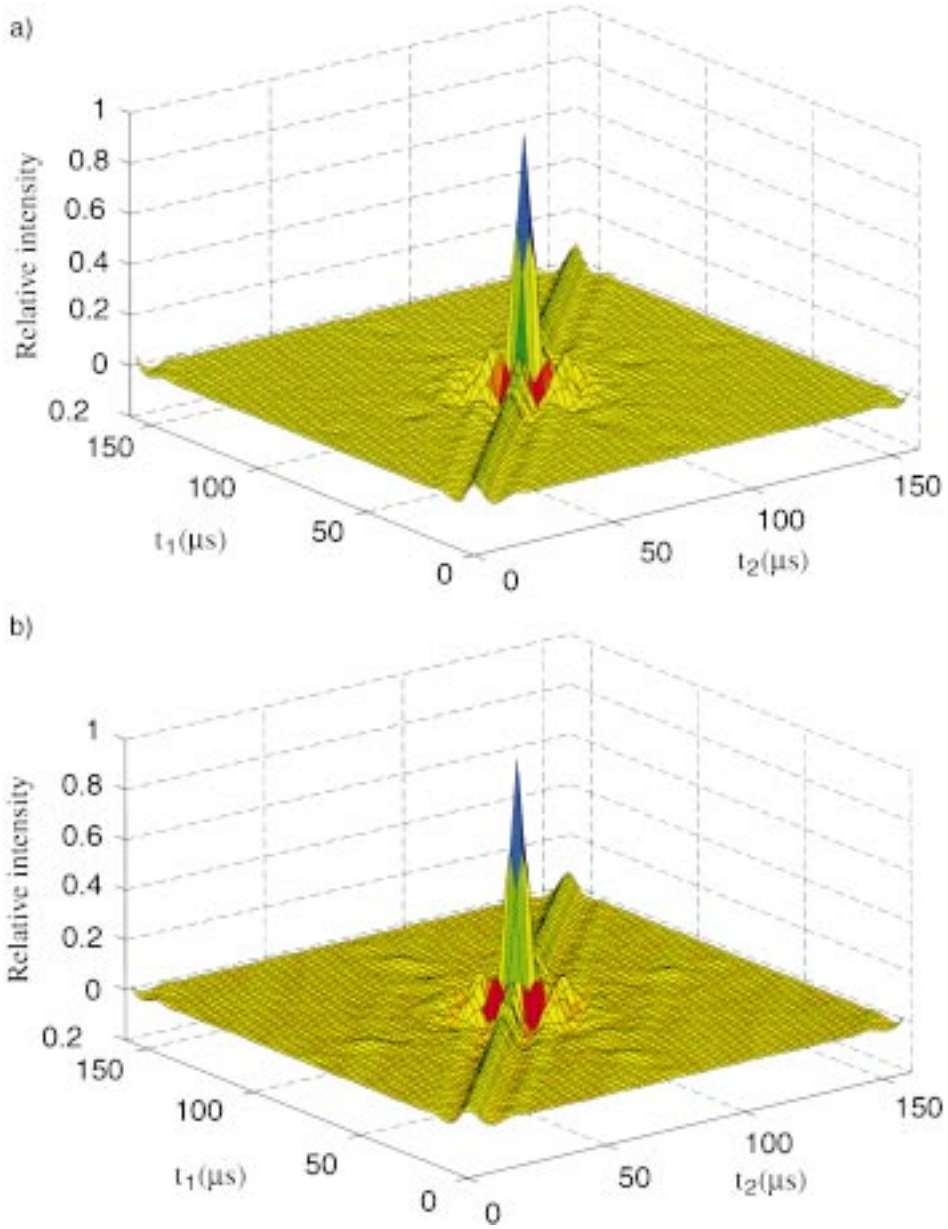

Fig. 4. a) *2D FID of the ^2H spin-diffusion experiment based on the pulse sequence of* Fig. 2 *with $\tau_m = 7$ s for the cyclo-β-peptide* **1**. b) *Computed pattern with $\theta_q = 15.7^\circ$ and $\phi_q = 72^\circ$ providing an optimum fit of* a.

Another prominent feature of the figure is an echo ridge extending along the diagonal $t_1 = t_2$. This is due to the refocusing of magnetization that has not exchanged with other ^2H atoms. The shape and oscillations near the central echo peak are found to be

sensitive to the mutual orientation of the quadrupolar tensors. According to *Eqn. 2*, the overall 2D signal has contributions from six possible spin pairs among the four magnetically non-equivalent ^{2}H atoms in a molecule. Since the two molecules per unit cell have identical angular orientation, spin diffusion between ^{2}H atoms on different molecules cannot be distinguished from that between ^{2}H atoms on the same molecule.

Based on *Eqns. 2*, *6*, and *7*, theoretical 2D spin-diffusion spectra have been computed and fitted to the experimental one by varying the orientation of the symmetry axis e_{S_4} defined by the angles θ_q^i and ϕ_{qr}^i. The best fit was obtained for $\theta_q^i = 15.7^\circ \pm 1.0^\circ$ and $\phi_q^i = \pm 72^\circ \pm 10^\circ$. The sign ambiguity in ϕ_q^i cannot be resolved based on quadrupolar tensor-correlation data. In addition, it is impossible, based on the measured data, to assign a particular tensor orientation to an (*R*)- or (*S*)-enantiomer. This leads to an additional possible value, $\theta_q^i = 164.3^\circ \pm 1.0^\circ$. The optimum theoretical 2D time-domain plot is shown in *Fig. 4,b*. To visualize the agreement of experimental results and simulated data, we plot the height of the diagonal echoes for $t_1 = t_2$. The solid line shown in *Fig. 5* is the experimental one from *Fig. 4,a*, while the crosses represent simulated 2D data for optimized θ and ϕ values.

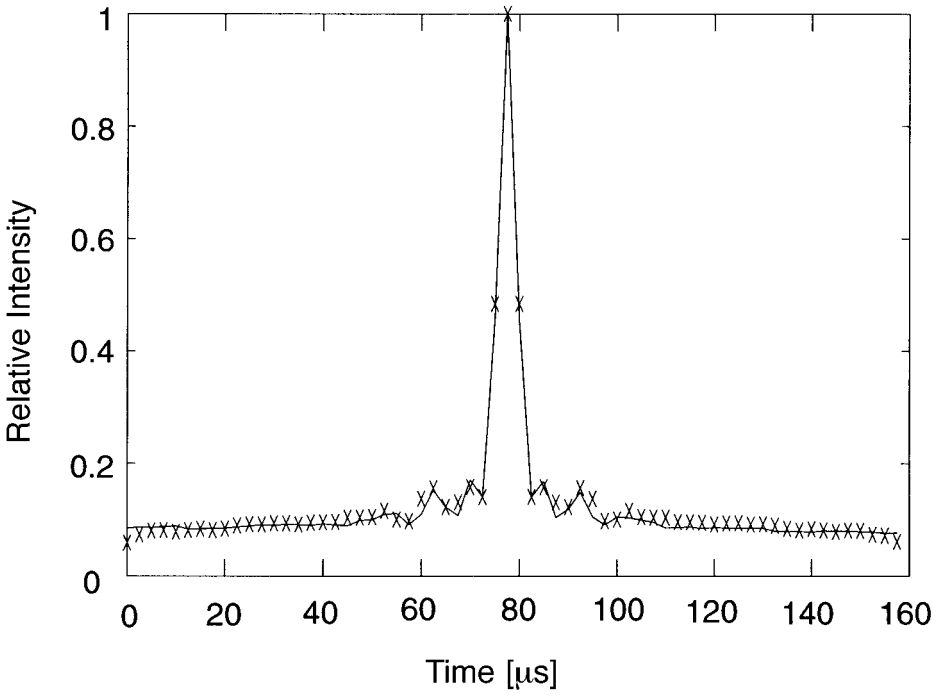

Fig. 5. *Diagonal section* ($t_1 = t_2$) *through the 2D FID in* Fig. 4, a. The crosses represent points of the computed 2D FID of *Fig. 4, b*.

Based on the four distinct sets of values for θ_q^i and ϕ_q^i, the backbone dihedral angles for the compatible peptide conformations were calculated by the numerical search method. For each set, two compatible conformations were found. The resulting angles are collected in *Table 1*. Stick models for the eight conformations are presented in *Fig. 6*.

Table 1. *Experimental Orientation Angles* θ_q^l *and* ϕ_q^l *of the* e_{S_t} *Symmetry Axis and Backbone Dihedral Angles* φ_1^1, φ_2^1, *and* ψ^1 *of Residue 1 of the Deduced Peptide Structures* (in degrees) *with the Corresponding Uncertainties Given as* ± *One Standard Deviation*

ϕ_q^1	θ_q^1	Structure	φ_1^1	φ_2^1	ψ^1
		I_A	176.7 ± 6.0	− 36.0 ± 5.0	− 76.0 ± 7.0
72 ± 10	15.7 ± 1.0	I_B	98.3 ± 4.0	36.0 ± 4.0	− 153.8 ± 4.0
		II_A	− 176.7 ± 6.0	36.0 ± 5.0	76.0 ± 7.0
− 72 ± 10	164.3 ± 1.0	II_B	− 98.3 ± 4.0	− 36.0 ± 4.0	153.8 ± 4.0
		III_A	176.7 ± 4.0	− 73.8 ± 1.0	− 36.6 ± 4.0
− 72 ± 10	15.7 ± 1.0	III_B	52.2 ± 5.0	73.8 ± 1.0	− 159.7 ± 3.0
		IV_A	− 176.7 ± 4.0	73.8 ± 1.0	36.6 ± 4.0
72 ± 10	164.3 ± 10	IV_B	− 52.2 ± 5.0	− 73.8 ± 1.0	159.7 ± 3.0
		X-ray	64	66	− 153

The *van der Waals* energies, computed for the eight conformations are given in *Table 2*. The three conformations III_A, IV_A, and IV_B are obviously strongly disfavored by steric hindrance and can be excluded due to their very high *van der Waals* energies. The most favorable conformation, regarding this measure, is II_A, but the values of II_B and III_B, are also reasonably low. It is tempting to select conformation II_A as the most likely one.

Table 2. *Structural Deviations from the X-Ray Structure and* van der Waals *Energies of the Eight Possible Conformations*

Structure	Dih. rmsd [degrees]	rmsd [Å]	*van der Waals* Energy[a]) [kJ/mol]
X-Ray	0	0	1188
I_A	88	2.28	3900
I_B	25	1.36	2123
II_A	90	2.08	976
II_B	99	1.76	1348
III_A	110	2.37	109×10^8
III_B	6	0.15	1432
IV_A	103	1.50	7075
IV_B	94	2.21	8845

[a]) *van der Waals* energies were computed with *Lennard-Jones* potential in *INSIGHT II 98.0* (*Molecular Simulations, Inc*. San Diego, CA) with *AMBER* force field [18][19].

For comparison with the NMR results, an X-ray powder-diffraction study (see *Table 3*) has been performed on the partially deuterated cyclo-β-peptide **1**. The nuclear coordinates are given in *Table 4*. The angular and distance rmsd values comparing the eight NMR structures with the X-ray structure are also contained in *Table 2*. They qualitatively correlate with the computed *van der Waals* energy. Extreme rmsd deviations from the X-ray structure for angles and for distances lead to extreme values of the *van der Waals* energy. The comparison verifies the proper selection of conformation III_B that is by an order of magnitude nearer to the X-ray structure than all other NMR conformations. This shows that the information obtained from the correlation of ^2H quadrupolar tensors is reliable and compatible with X-ray data.

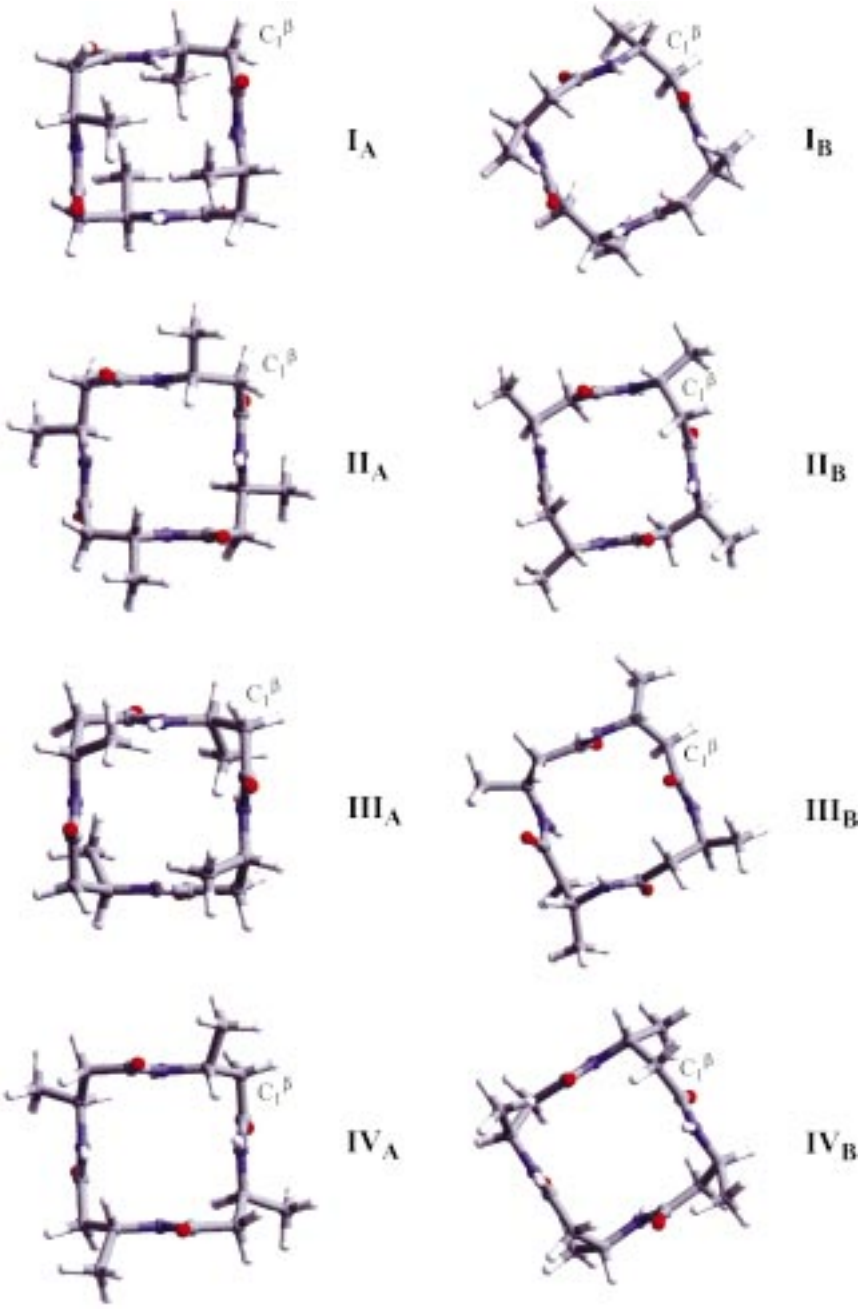

Fig. 6. *Stick models of the eight molecular conformations of the cyclo-β-peptide* **1** *corresponding to the dihedral angles in* Table 1

Table 3. *Experimental and Crystallographic Data for the Partially Deuterated Cyclo-β-peptide Cyclo[(S)-β-homoalanyl-(R)-β-homoalanyl-(S)-β-homoalanyl-(R)-β-homoalanyl]*

Data Collection	
Instrument	*Stoe STADI P*
Wavelength	Cu$K_{\alpha 1}$
2θ Range [°2θ]	7.5 – 65
Step size [°2θ]	0.02
Unit Cell	
Space group	$I\bar{4}$
a [Å]	13.6354(2)
c [Å]	4.8836(1)
Refinement	
Standard peak for peak shape function [hkl, °2θ]	*110*, 9.165
Peak range (No. of *FWHM*)	20
No. of observations (steps, N)	2875
No. of contributing reflections	80
No. of geometrical restraints	44
No. of non-H(D) structural parameters ($P1$)	21
No. of H(D) structural parameters ($P2$)	12
No. of profile parameter	7
$R_F = \Sigma \lvert F_{obs} - F_{calc} \rvert / \Sigma F_{obs}$	0.060
$R_{wp} = \{\Sigma w[y_{obs} - y_{calc}]^2 \mid \Sigma w y^2_{obs}\}^{1/2}$	0.122
$R_{exp} = [(N - P1 - P2)/\Sigma w y^2_{obs}]^{1/2}$	0.091

Table 4. *Fractional Coordinates and Displacement Parameters for the Partially Deuterated Cyclo-β-peptide Cyclo[(S)-β-homoalanyl-(R)-β-homoalanyl-(S)-β-homoalanyl-(R)-β-homoalanyl]*[a])

Atom	x	y	z	U_{iso} [Å^2]
C(1)=O	0.322(2)	0.415(2)	0.505(5)	0.032[b])
C(2)H_2	0.360(2)	0.320(3)	0.388(5)	0.032[b])
C(3)–H	0.260(2)	0.578(2)	0.407(4)	0.032(2)[b])
C(4)H_3	0.1546(5)	0.562(1)	0.512(4)	0.115(8)[c])
O	0.307(1)	0.4230(9)	0.755(2)	0.032[b])
N	0.306(1)	0.486(1)	0.328(3)	0.032[b])
H^{Si}–C(2)	0.41(1)	0.34(1)	0.21(3)	0.10
H^{Re}–C(2)	0.30(1)	0.27(2)	0.32(8)	0.10
H–C(3)	0.25(1)	0.623(9)	0.22(2)	0.10
^{2}H–N	0.32(1)	0.475(8)	0.13(2)	0.10

[a]) Numbers in parentheses are the esd's in the units of the last significant digit given. Parameters without esd's were held fixed in refinement. The coordinates are given for an (*R*)-enantiomer.

[b]) Parameters were constrained to be equal.

[c]) The population parameter for this C-atom was set to 1.5 to simulate a Me group. The coordinates of the Me protons have not been determined.

Conclusion. – It should be admitted that a full structure determination of the cyclo-β-peptide **1** by ^{2}H spin-diffusion spectroscopy was feasible only due to the particularly favorable circumstance that the molecule has S_4 symmetry. The measurement of just a pair of orientational angles permitted the determination of eight feasible conformations, among which a simple *van der Waals* energy consideration allowed the selection of the proper conformation. It agrees within an angular rmsd of 6° and a distance rmsd of 0.15 Å with the structure determined by X-ray powder diffraction.

For less symmetric or more complex molecules, additional information could be obtained by selective ^2H labeling, and the same measurement and analysis procedure or, possibly, by non-selective labeling and fitting an overlap of non-equivalent spin-diffusion patterns. It is apparent that both procedures have their inherent limitations. It is more likely that the information obtained from the orientational correlation of ^2H quadrupolar tensors is useful in combination with data obtained from other sources, for example, from the correlation of ^{13}C chemical-shielding tensors [12] or of dipolar-coupling tensors [10] or from a combination of both [11].

Solid-state NMR is inherently a powerful technique for the study of molecular conformations of molecules that cannot be dissolved or that change their structure upon dissolving. But the information is invariably limited and any additional source of information, such as the mutual orientation of ^2H quadrupolar-coupling tensors, discussed in the present paper, is valuable.

This work was supported by *Swiss National Science Foundation*. *H.C.L.* was supported by a *Human Frontier Science Program* fellowship. Helpful discussions with Dr. *Pierre Robyr* are gratefully acknowledged. We thank Dr. *Jennifer L. Matthews* for constructive comments in the preliminary phase of the study.

Experimental Part

Sample Preparation. The cyclo-β-tetrapeptide **1** ($^1H_4$ instead of $^2H_4$) was synthesized by cyclization of the corresponding open-chain β-tetrapeptide, as described in [16][20]. The non-labeled cyclo-β-peptide precipitates from the cyclization-reaction soln. It was then dissolved in CF_3CO_2D/CH_2Cl_2 1:1 for H/^{2}H exchange. The deuterated cyclo-β-tetrapeptide was recrystallized three times from MeCN (0.4% D_2O) for purification and to ensure formation of crystalline domains necessary for X-ray diffraction. The sample purity was checked by high-resolution ^{1}H-NMR spectroscopy.

^{2}H-NMR Measurements. 2D FIDs were acquired with the pulse sequence shown in *Fig. 3*. The sensitivity was enhanced by ^{1}H-^{2}H variable-amplitude cross polarization [21]. NMR Experiments were performed on a home-built 300-MHz solid-state spectrometer at r.t. ^{1}H-^{2}H Double-resonance measurements were carried out with a *Chemagnetics* 6-mm double resonance probe (*Varian*, Fort Collins, CO, USA). The sample was spun at 6.25 kHz. A spinning-speed stability of ± 1 Hz was achieved by using a *Chemagnetics* spinner frequency controller (*Varian*, Fort Collins, CO, USA). A proton RF field of 35 kHz was used for cross polarization and decoupling. The mixing time τ_{cp} for ^{1}H-^{2}H cross polarization was 5 ms, and the mixing time for ^{2}H spin diffusion τ_m was set to 7 s. The RF power on the ^{2}H channel during cross polarization was ramped through the optimum ^{2}H RF field strength. The 90° pulse length for ^{2}H was 3 μs. The time increments for both t_1 and t_2 dimensions were 2.5 μs. 64 t_1 Increments were used, and 64 scans were accumulated for each t_1 increment. The total acquisition time for a full measurement was *ca*. 12 h.

Data Analysis and Processing. The 2D time-domain data were processed with the program package *Felix* (*MSI*, San Diego, CA, USA) and then analyzed by simulating the correlation spectra for a ^{2}H pair with variable relative orientation of the two quadrupolar tensors.

Due to the wide ^{2}H spectra, it was not possible to homogenously cross-polarize the entire frequency range. The limited experimental excitation window was taken into account by convoluting the computer-simulated 2D FID $g'(i,j)$ with a weighting function $h(i,j)$ with

$$h(i,j) = \begin{cases} 1, & \text{for } i = j \\ x, & \text{for } i = j \pm 1 \\ 0, & \text{for } |i-j| > 1 \end{cases} \tag{10}$$

before comparing with the experimental FID $f(i,j)$:

$$g(i,j) = \sum_{m,n=1}^{3} h(i+m,j+n) \cdot g'(i+m,j+n). \tag{11}$$

The scaling factor x was determined by comparing two 1D ^{2}H spectra, one obtained by a single-pulse excitation (*Fig. 7,a*) and the other by cross-polarization excitation (*Fig. 7,b*). The value $x = 0.118$ was found. The

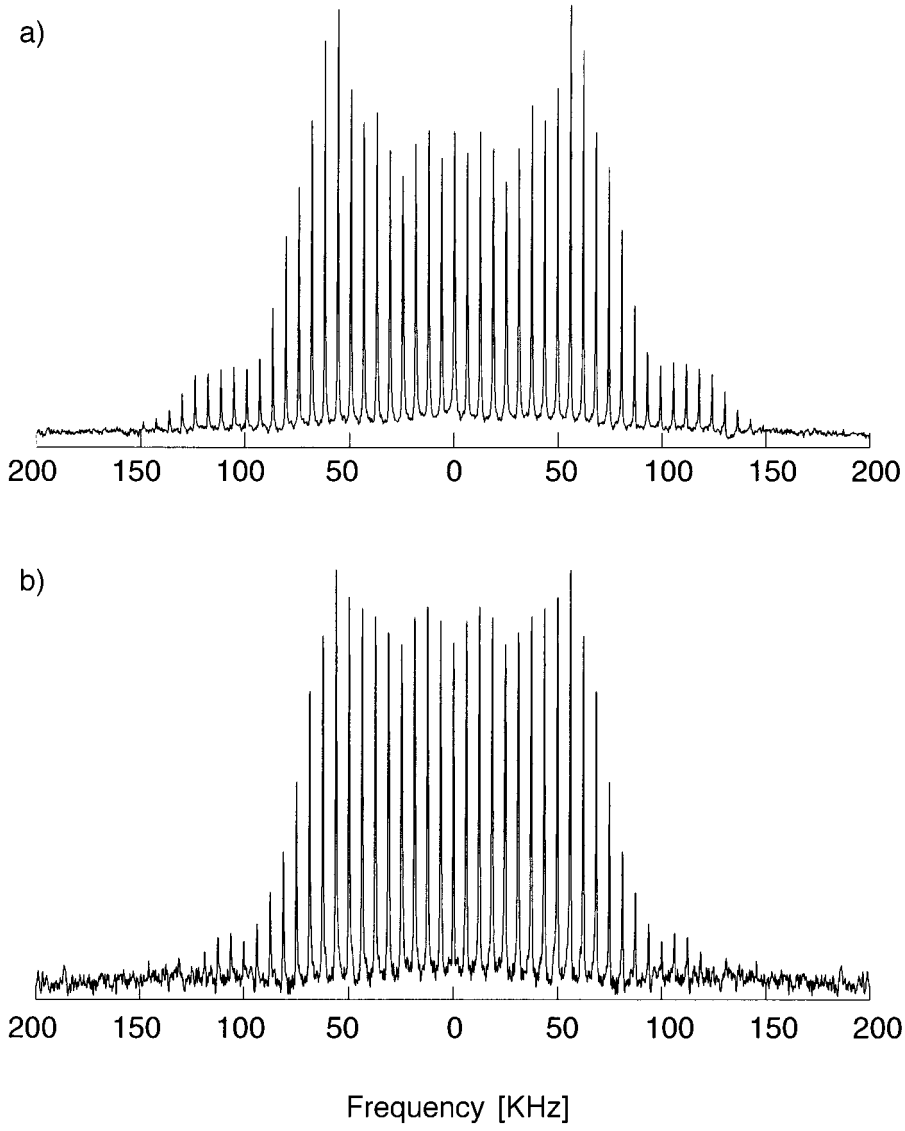

Fig. 7. *1D ^2H Spectra of cyclo-β-tetrapeptide* **1**. *a*) Obtained after a 90° pulse with pulse length 3.0 μs. *b*) Obtained after ^1H-^2D cross-polarization. The mixing time for cross-polarization is 5 ms.

quadrupolar coupling constant $Q_c = 190 \pm 5$ kHz and the assymmetry parameter $|\eta| = 0.20 \pm 0.02$ were also determined by fitting 1D ^2H spectra.

The deviation χ^2 between experimental and simulated spectra,

$$\chi^2 = \sum_{t_1,t_2} (f(t_1,t_2) - g(t_1,t_2))^2, \tag{12}$$

was minimized by an optimal orientation θ_q^i and ϕ_q^i of the molecular symmetry axis e_{S_4} in the quadrupolar principle-axis frame of residue 1 by means of MATLAB routines (*Math-Works, Inc.*, Natick, MA, USA).

Molecular coordinates were generated from the optimized set of angles by means of home-written MATLAB programs with bond lengths and bond angles from the program package *XRS-82* [22].

X-Ray Crystallography. X-Ray powder-diffraction data were collected on the partially deuterated cyclo-β-peptide in transmission mode (0.3 mm rotating capillary) on a high-resolution laboratory diffractometer (*Stoe STADI P*) with CuK_{α_1} radiation. Further details of the data collection are given in *Table 3*.

Comparison of the powder-diffraction pattern collected on the partially deuterated material with that collected previously [16] on the non-labeled compound proved both materials to be very similar. However, to verify this, *Rietveld* refinement was performed by means of the program package XRS-82 [22]. Two refinements were initiated, one with the atomic coordinates from the structure refinement of the non-labeled cyclo-β-peptide [16] and a second one with the same molecular-packing model but the conformational geometry III_B of the NMR analysis. For the two starting models, the same refinement procedure was applied. Strong restraints on bond distances and angles were used during the initial stage of refinement to maintain the chemical sense of the molecule. Additional restraints were imposed to keep the amide moieties planar. To approximate the contribution from the H-atoms of the Me groups, the population parameter of the respective C-atom was increased from 1.0 to 1.5 (six electrons for the C- and one for each of the three H-atoms). The relative weight of the geometric restraints with respect to the X-ray data was gradually reduced as the refinement proceeded. However, complete removal of the restraints resulted in somewhat unsatisfying interatomic distances and angles, so they were retained. Two displacement factors were refined one for C(Me) and a second for the remaining non-H atoms.

Within the standard deviation of the structural parameters, the final refinement of the two models converged in the same minimum with $R_F = 0.060$ and $R_{wp} = 0.122$ ($R_{exp} = 0.091$). Further details of the refinement are given in *Table 3*. The structural parameters for the refinement starting from the NMR model are listed in *Table 4*, and the observed and calculated powder patterns are shown in *Fig. 8*. The backbone dihedral angles, calculated with the program BONDLA [23], are included in *Table 1*.

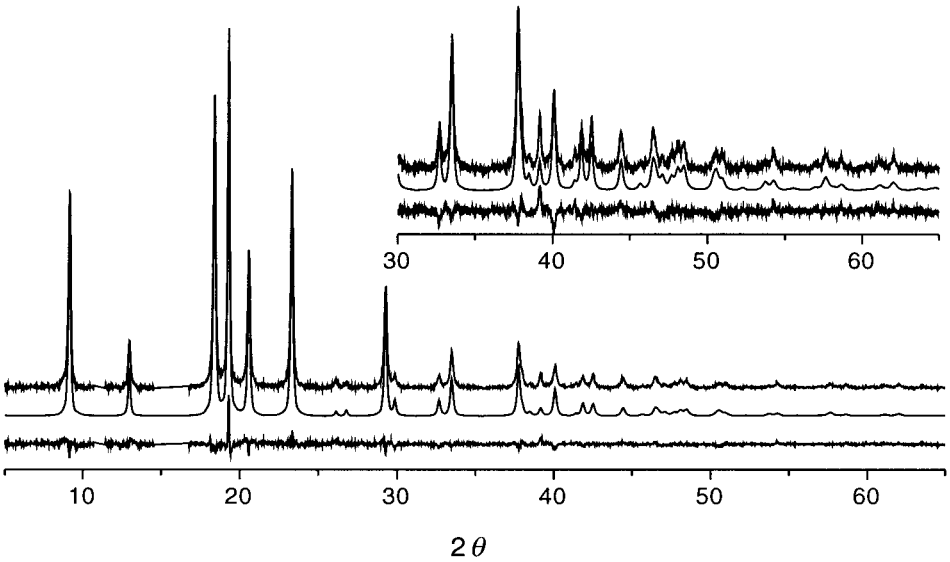

Fig. 8. *The observed* (top), *calculated* (middle), *and difference* (bottom) *profiles for the* Rietveld *refinement of the partially deuterated cyclo-β-peptide cyclo[(*S*)-β-homoalanyl-(*R*)-β-homoalanyl-(*S*)-β-homoalanyl-(*R*)-β-homoalanyl]* (**1**). The intensity scale for the inset has been increased by a factor of 3 to show more detail.

REFERENCES

[1] K. Wüthrich, 'NMR of Proteins and Nucleic Acids', John Wiley & Sons, New York, 1986.
[2] R. R. Ernst, G. Bodenhausen, A. Wokaun, 'Principles of Nuclear Magnetic Resonance in One and Two Dimensions', Clarendon Press, Oxford, 1987.
[3] 'Biological NMR Spectroscopy', Eds. J. L. Markley, S. J. Opella, Oxford University Press, New York, 1997.
[4] 'Protein NMR Techniques' in 'Methods in Molecular Biology', Ed. D. G. Reid, Humana Press, Totowa, New Jersey, 1997, Vol. 60.
[5] D. Neuhaus, M. P. Williamson, 'The Nuclear Overhauser Effect in Structural and Conformational Analysis', Wiley-VCH, Weinheim, 2000.
[6] D. P. Raleigh, M. H. Levitt, R. G. Griffin, *Chem. Phys. Lett*. **1988**, *146*, 71.
[7] R. Tycko, G. Dabbagh, *Chem. Phys. Lett*. **1990**, *173*, 461.
[8] A. E. Bennett, R. G. Griffin, S. Vega, 'Recoupling of Homo- and Heteronuclear Dipolar Interactions in Rotating Solids' in 'NMR Basic Principles and Progress', Ed. B. Blümich, 1994, Vol. 33, p. 1.
[9] T. Gullion, J. Schaefer, *J. Magn. Reson*. **1989**, *81*, 196.
[10] X. Feng, M. Eden, A. Brinkmann, H. Luthman, L. Eriksson, A. Graslund, O. N. Antzutkin, M. H. Levitt, *J. Am. Chem. Soc*. **1997**, *119*, 12006.
[11] D. P. Weliky, G. Dabbagh, R. Tycko, *J. Magn. Reson., Ser. A* **1993**, *104*, 10.
[12] M. Tomaselli, P. Robyr, B. H. Meier, C. Grob-Pisano, R. R. Ernst, U. W. Suter, *Mol. Phys.* **1996**, *89*, 1663.
[13] K. Takegoshi, M. Ito, T. Terao, *Chem. Phys. Lett*. **1996**, *260*, 159.
[14] Z. Gan, P. Robyr, R. R. Ernst, *Chem. Phys. Lett*. **1998**, *283*, 262; Z. Gan, P. Robyr, *Mol. Phys*. **1998**, *85*, 1143.
[15] D. Seebach, P. E. Ciceri, M. Overhand, B. Jaun, D. Rigo, L. Oberer, U. Hommel, R. Amstutz, H. Widmer, *Helv. Chim. Acta* **1996**, *79*, 2043; D. Seebach, J. L. Matthews, *Chem. Commun*. **1997**, 2015.
[16] D. Seebach, J. L. Matthews, A. Meden, T. Wessels, C. Baerlocher, L. B. McCusker, *Helv. Chim. Acta* **1997**, *80*, 173.
[17] R. Gerald II, T. Bernhard, U. Haeberlen, J. Rendell, S. Opella, *J. Am. Chem. Soc*. **1993**, *115*, 777.
[18] S. J. Weiner, P. A. Kollman, D. A. Case, U. C. Singh, C. Ghio, G. Alagona, S. Profeta Jr., P. Weiner, *J. Am. Chem. Soc*. **1984**, *106*, 765.
[19] S. J. Weiner, P. A. Kollman, D. T. Nguyen, D. A. Case, *J. Comp. Chem.* **1986**, *7*, 230.
[20] J. L. Matthews, M. Overhand, F. N. M. Kühnle, P. E. Ciceri, D. Seebach, *Liebigs Ann. Chem.* **1997**, *7*, 1371.
[21] P. K. Madhu, Department of Chemical Physics, Weizmann Institute of Science, Rehovot 76100, Israel, personal communication.
[22] C. Baerlocher, 'XRS-82. The X-ray Rietveld System', ETH-Zürich, 1982.
[23] W. Dreissig, R. Doherty, J. Steward, S. Hall, 'BONDLA', in 'Xtal 3.2. Reference Manual'. Eds. S. R. Hall, H. D. Flack, J. M. Steward, Universities of Western Australia, Geneva, and Maryland.
[24] Z. H. Gan, R. R. Ernst, *Solid State Nucl. Magn. Reson.* **1997**, *8*, 153.

Received October 20, 2000